



Kinetics and Thermodynamics of Sorption of 4-Nitrophenol on Activated Kaolinitic Clay and *Jatropha Curcas* Activated Carbon from Aqueous Solution

Samsudeen Olanrewaju Azeez¹ and Folahan Amoo Adekola^{2*}

¹Chemistry Unit, Department of Chemical, Geological and Physical Sciences, Kwara State University Malete, P.M.B. 1530, Ilorin, Nigeria.

^{2*}Department of Industrial Chemistry, University of Ilorin, P.M.B 1515, Ilorin 240222, Nigeria.

*Corresponding Author Email: faadekola@yahoo.fr

Received 26 January 2016, Revised 03 June 2016, Accepted 06 June 2016

Abstract

Adsorption behaviour of 4-nitrophenol (4-NP) on activated kaolinitic clay and *Jatropha curcas* activated carbon was investigated. The kaolinitic clay and *Jatropha curcas* were activated with 1 M HNO₃ and 0.5 M NaOH respectively and were characterized by XRF, XRD, BET, SEM and FTIR techniques. The effects of processing parameters, such as initial 4-NP concentration, temperature, pH, contact time and adsorbent dosage on the adsorption process were investigated. The results obtained showed that *Jatropha curcas* activated carbon exhibited higher performance than activated kaolinitic clay for the removal of 4-nitrophenol from aqueous solution. Langmuir, Freundlich, Temkin and Dubinin-Radushkevich models were used to describe the adsorption isotherms. The adsorption data were best fitted with Freundlich model. The experimental data of the two adsorbate-adsorbent systems fitted very well with the pseudo-second order kinetic model with r^2 values of 0.999 respectively. Adsorption thermodynamic parameters were also estimated. The results revealed that the adsorption of 4-nitrophenol onto both adsorbents were exothermic processes and spontaneous for *Jatropha curcas* activated carbon but non spontaneous for activated kaolinitic clay.

Keywords: 4-nitrophenol; Adsorption isotherm; *Jatropha curcas*; Kaolinitic clay; Kinetics; Thermodynamics.

Introduction

Organic pollutants such as 4-nitrophenol and other phenolic compounds usually abound in wastewaters discharged from oil refinery, plastic manufacturing industries, pharmaceutical industries, coke plants and phenolics resin plants [1]. Because of their high volatility and solubility, phenol and its compounds impart taste and odour on water even at parts per billion levels. Phenol is protoplasmic poison and so it damages all kind of cells. Hence, there is a need to remove phenolics waste effluent generated from these industries before discharging it into the environment [2, 3]. Various treatment technologies have been reported to remove these contaminants from wastewaters such as steam distillation [4], chemical extraction

[5], separation membrane [6, 7], air oxidation [8, 9], electrochemical oxidation [10-13] and biochemical abatement [14]. Many problems associated with the above mentioned methods include high cost, low efficiency and generation of toxic products [15]. However, adsorption has been chosen as one of the most widely acceptable effective techniques to remove phenolic at this concentration due to its relatively simple design, cost effectiveness, ease of operation and simple regeneration [16, 17]. A good number of adsorbents have been reported by researchers for wastewater treatment and remediation. Some include the adsorption of phenol on natural clay reported by Djebbar *et al.* [18], the equilibrium

kinetic and thermodynamic studies on the adsorption of phenol onto activated phosphate rock reported by Atef and Waleed [19]. Preeti and Singh [20] also investigated the sorption of phenol and p-nitrophenol from aqueous solution using clay sorbent. In addition, Adegoke and Adekola [21] investigated the removal of phenol from aqueous solution by activated carbon prepared from some agricultural materials and Hatem *et al.* [22] reported the isotherms, kinetics and thermodynamics of 4-nitrophenol adsorption on fiber-based activated carbon from coconut husks prepared under optimized conditions. Consequently, as a result of growing interest in the use of low cost adsorbents for wastewater treatment and remediation. It becomes imperative to activate the natural indigenous adsorbent by natural or synthetic materials.

Kaolinitic clay is clay that is rich in kaolinite also known as china clay [23]. They are parts of the group of industrial minerals with chemical composition $Al_2Si_2O_5(OH)_4$. It is a layered silicate mineral with one tetrahedral sheet linked through oxygen atoms to one octahedral sheet of alumina [24]. It has many uses due to its favourable properties such as natural whiteness, fine particle size, non-abrasiveness, and chemical stability. It is applied in the production of rubber, plastics and pigments as filler and also for the production of synthetic zeolites and thus, as an adsorbent in drugs [25]. *Jatropha curcas* is one of the species of flowering plant in the genus *Jatropha* in spurge family, Euphorbiaceae, a tropic plant of Mexico and Central America [26]. The seeds contain 27- 40% oil (average: 34.4%) that could be processed to produce a high-quality biodiesel fuel, usable in a standard diesel engine [27, 28]. The seed coat is hard which allows it to be charred and used as an adsorbent.

The prime objective of this study was to investigate the removal of 4-NP from aqueous solution by activated Kaolinitic (AKC) clay and *Jatropha curcas* activated carbon (JAC) with a view to determining their efficacy and effectiveness. The effects of initial 4-NP concentration, pH, contact time, and adsorbent dosage on adsorption capacity were investigated.

Kinetic models and thermodynamic parameters were tested on the experimental data and their constants determined.

Materials and Methods

Reagents and apparatus

The reagents and chemicals that were used for this experiment were of analytical grade as follows: 4-nitrophenol (BDH, 98%, Prd. No: 30167), hydrochloric acid (Purity 37%, density 1.1 kg/cm³, Riedel-deHaen, Buffalo, NY, USA), sodium hydroxide (BDH prod. No. 30167, Sigma Aldrich, Diegem, Belgium) and Nitric acid (purity 98%, 1.51gcm³), were used without further purification.

Sample collection and preparation of the adsorbents

The Kaolinitic clay sample that was used for this experiment was sourced from Batagbon mining site in Kwara State, Nigeria. The *Jatropha curcas* fruit used was collected from private estates in Ilorin, Nigeria. The seed coat was used for the preparation of activated carbon. The Kaolin clay sample was ground and sieved into particle size < 90 µm using Tyler screen standard sieves. It was then soaked in concentrated HCl solution for 4hr. to eliminate impurities and further washed severally with deionised water and oven-dried [19]. The *Jatropha curcas* seed coat was carbonised at a temperature of 500 °C for 1hr 30min and ground into smaller sizes, and also sieved into particle size, < 90 µm [21]. 100 g of the sieved clay (< 90 µm) was activated with 1 M nitric acid by adding 400 mL of the acid solution and stirred on a magnetic stirrer at affixed rate of 500 rpm for 2 hr 30 min at a temperature of 90°C. The sample was then filtered, washed severally with deionized water to neutral pH and dried at 105°C to obtain activated kaolinitic clay (AKC) sample [20]. The sieved carbon prepared from *Jatropha curcas* seed coat was activated with 0.5 M NaOH. 50 g of the *Jatropha curcas* was impregnated into 200 mL of 0.5 M NaOH solution for 48 hours. The sample was then filtered, washed with deionized water to neutral pH and oven-dried at 105°C [21].

Characterization of the adsorbents

The mineralogical composition of the kaolinitic clay sample was carried out using MINI PAL4 EDXRF Spectrometer. The X-ray diffraction (XRD) of the kaolinitic clay was carried out using a PANalytical X'Pert PRO MRD PW3040 model. The surface area of both AKC and JAC were examined by Brunauer, Emmet and Teller (BET) analysis of N₂ adsorption at 77K using Micromeritics ASAP 2020 V3.02H model. The surface morphology of the adsorbents were analysed using the scanning electron microscope (SEM) model ASPEX 3020. Fourier transform infrared spectroscopy (FTIR, Shimadzu, Columbia, MD, USA) absorption spectra were obtained using the potassium bromide (KBr) pellet method and the spectra of the samples were recorded over the range 4000–400 cm⁻¹ using Shimadzu FTIR-8400S.

Preparation of standard solution

A stock solution of 4-NP (1000 mg/L) was prepared by dissolving 1.0 g of the adsorbate with deionized water in 1000 mL capacity standard volumetric flask and serial dilution was made to obtain other lower concentrations required [20].

Adsorption experiment

The adsorption experiment was carried out by batch equilibrium method. The experiment involved preparing 20 mL of different concentrations of 4-NP and contacted with 0.2 g (AKC) and 0.02 g (JCA) in a 100 mL conical flasks. The content was agitated for 2 hr at 200 rpm at a temperature of 28±2°C. The pH of the solution was adjusted using 0.1 M HCl or 0.1 M NaOH solutions by a pH meter model. The effect of experimental parameters such as pH, contact time, adsorbent dosage (AKC and JAC) and temperature were studied. The solutions were then centrifuged at 10,000 rpm for 10 min and the supernatant solution filtered and analysed using a UV/Visible spectrophotometer (Bechman Coulter DU 730 Pasadena, CA, USA) at λ_{max} of 400 nm for 4-NP. The amounts of 4-NP adsorbed, q_e (mg/g) and % 4-NP adsorbed were calculated using equation 1 and 2 [22, 29-30]:

$$q = \frac{(C_o - C_e)V}{W} \quad (1)$$

$$\% \text{ 4-NP adsorbed} = \frac{(C_o - C_e)}{C_o} \times 100 \quad (2)$$

Where; C₀ and C_e are the initial and equilibrium concentration of 4-NP (mg/L), V is the volume of the solution (L) and W is the amount of adsorbent used (g).

All experiments were performed in triplicate to ensure the reproducibility of the results; the mean of the measurements was reported.

Results and Discussion

Composition of the kaolinitic clay

The mineralogical composition of the kaolin sample is depicted in the Table 1.

The major compounds detected by the XRF are Al₂O₃ (43.3%) and SiO₂ (52.0%) as in Table 1. High grade Kaolin samples have been found to contain Al₂O₃ (alumina) in the range (33 – 42%) [31].

Table 1. Chemical composition of kaolinitic clay sample by XRF.

Compo unds	Al ₂ O ₃	Si O ₂	K ₂ O	CaO	Ti O ₂	Fe ₂ O ₃	Mn O	Cr ₂ O ₃	V ₂ O ₅	Ag ₂ O
Conc. %	43.3	52.0	0.041	0.214	1.68	1.04	0.016	0.036	0.085	1.40

X-ray diffraction (XRD) of the kaolinitic clay

Fig. 1 clearly shows that AKC has intense peaks at 2θ values of 12.5°, 24.9° and 62.3° with less intense peaks at 2θ values of 19.8°, 35.9°, 37.7°, and 38.4° which are characteristics of kaolinite and this complement the result of the chemical analysis. The spectrograph also shows the diffraction peaks of quartz at 2θ values of 20.9°, 26.7° and 50.1° using International Card for Diffraction Data (ICDD) as reference and this result corresponds with the JCPDS file no 01-078-1996 and 01-079-1910 for kaolinite and quartz respectively [32].

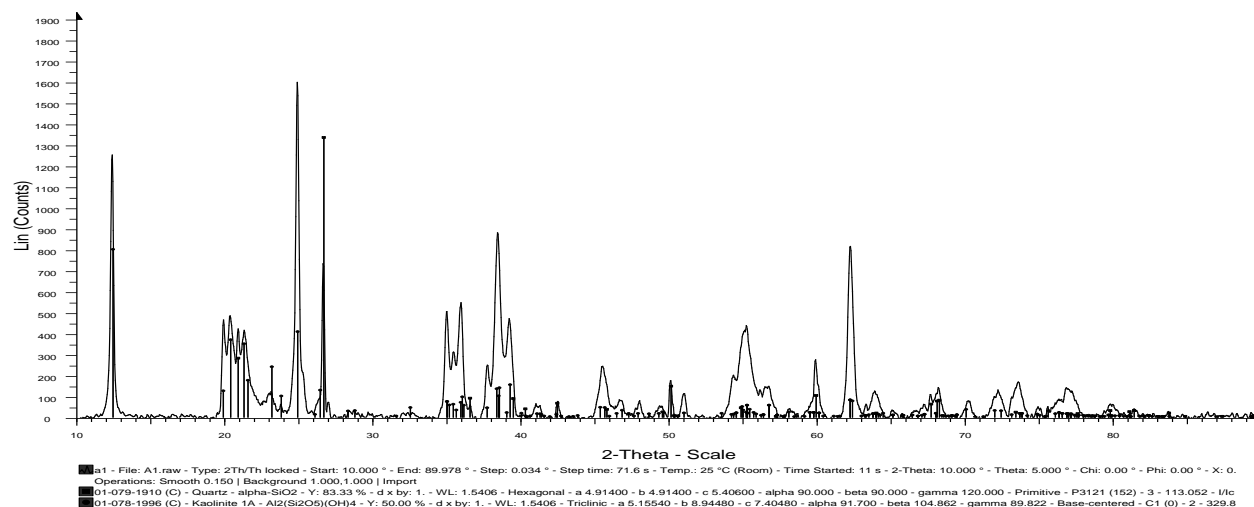


Figure 1. XRD patterns of AKC

Surface area determination of the adsorbents

The results of the surface area analysis of the adsorbents are tabulated in Table 2. Summarily, the BET surface area and pore volume of JAC is significantly higher than AKC while the pore size of AKC is greater than JAC. According to the classification by International Union of Pure and Applied Chemistry [33], pores are classified as micropores (< 2nm diameter), mesopore (2-50 nm diameter) and macropores (> 50 nm diameter). It can be seen Table 2 that both AKC and JAC are composed mainly of mesopores with surface area in the range of 20 to 100 m² per gram and pore size of about 3.4 nm and 2.1 nm respectively. The larger surface area and pore volume recorded for JAC viz-a-viz the pore size in the mesopore region suggest that JAC might be a better adsorbent in the uptake of 4-NP.

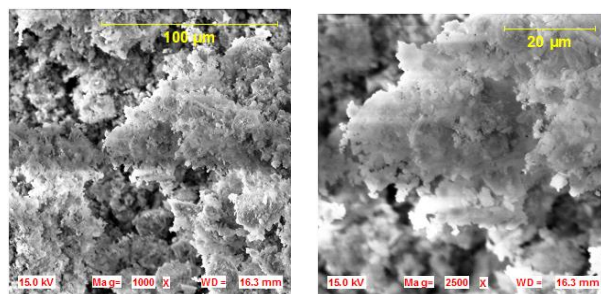
Table 2: BET results of the Adsorbents.

Adsorbents	BET surface area (m ² /g)	Pore volume (cm ³ /g)	Pore size (nm)
AKC	20.60	0.0180	3.480
JAC	50.30	0.026	2.10

Scanning electron microscopy (SEM)

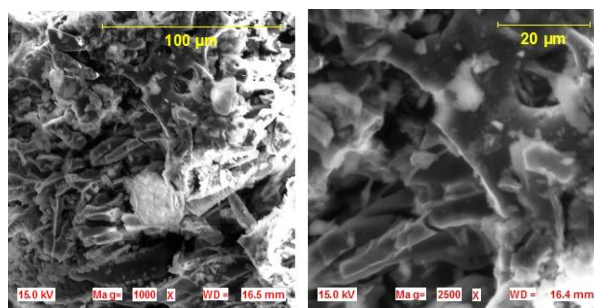
The SEM images of AKC and JAC are presented in Fig. 2. The SEM image of AKC (Fig. 2a-b) shows the microstructure of the adsorbent are composed of platelets, which aggregated into a

larger size mesoporous particle that are not evenly distributed. The SEM micrographs of JAC (Fig. 2c-d) at different magnifications showed lamellar stratified surface and indicates cavities, pores and more rough surfaces on the carbon sample with several large clusters of mesopores spotted on it which revealed that it is highly porous and this is similar to what was earlier reported by Karthikeyan *et al.* [34].



a. AKC (mag 1000x)

b. AKC (mag 2500x)



c. JAC (mag 1000x)

d. JAC (mag 2500x)

Figure 2. SEM images of the adsorbents

Fourier transform infra-Red spectroscopy (FTIR)

The results of the FTIR spectra of ACK and JAC before and after adsorption were presented in Fig 3a-d. The FTIR spectra of ACK (Fig. 3a) revealed the characteristic bands of kaolinite appearing at 3695 cm^{-1} , 3655 cm^{-1} , 3620 cm^{-1} and 3585 cm^{-1} attributed to the stretching vibrations of the surface hydroxyl groups (Si-Si-OH, or Al-Al-OH). The band observed at 3460 cm^{-1} and 3437 cm^{-1} were assigned to O-H stretching vibrations of adsorbed water molecules. The peak at 2359 cm^{-1} represents Si-H vibrations while the band at 1101 cm^{-1} was attributed to Si-O

stretching. The bands at 914, 793, 652 and 432 cm^{-1} were assigned to Si-O-Al and Si-O-Fe bending vibrations respectively. This indicated that most part of the layer charge resulted from trivalent (Al^{3+} and Fe^{3+}) ion substitution in the octahedral sheet. These functional groups are commonly found in silicate minerals such as kaolinite [35, 36]. Fig. 3b revealed the evidence of 4-NP interactions with AKC due to spectral changes and shift of prominent peaks from 3460 cm^{-1} to 3446 cm^{-1} due to phenolic O-H vibration stretching and also shifting of prominent kaolinite vibrations were observed at 1008 cm^{-1} , 1031 cm^{-1} and 1105 cm^{-1} due to C-N stretching.

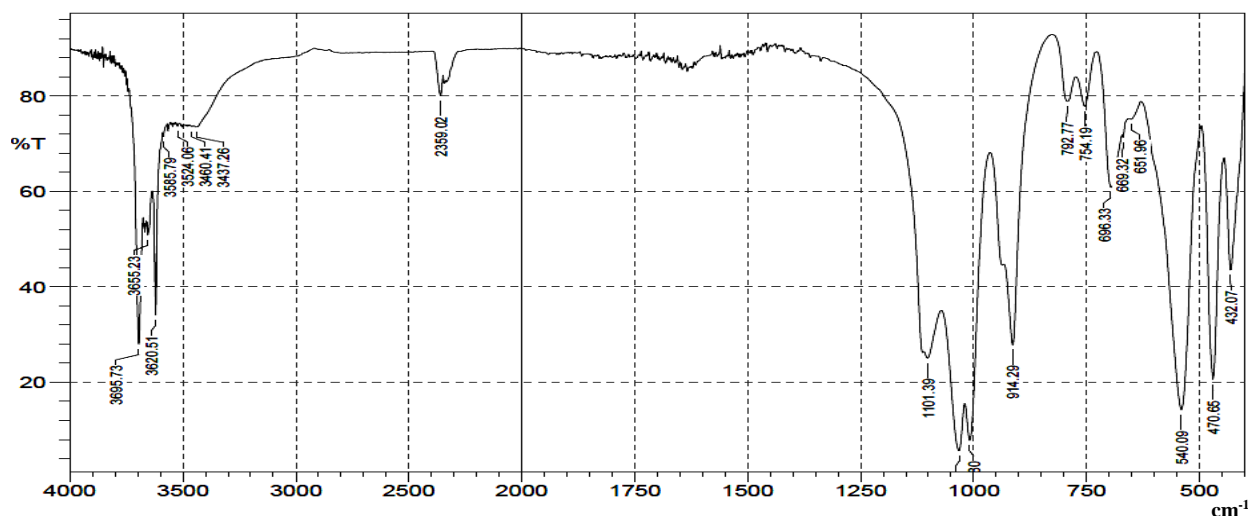


Figure 3a. FTIR Spectra of AKC (before adsorption)

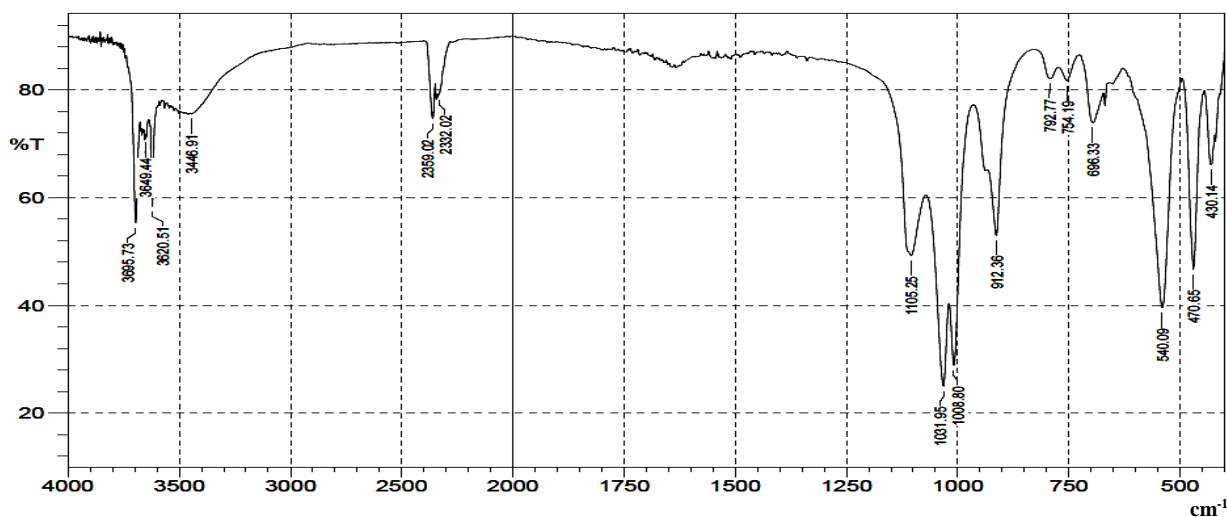


Figure 3b. FTIR spectra of AKC after adsorption with 4-NP

Fig. 3c is the FTIR spectrum of JAC before adsorption. This figure shows a strong broad absorption peak at 3399 cm^{-1} representing O-H vibration stretching. The band recorded in the region of 1574 cm^{-1} corresponds to C=C stretch. There was a peak at 1373 cm^{-1} due to C-O-H bending. Other important absorption bands at 1038 cm^{-1} represent C-O stretch of primary alcohol of lignin and 1111 cm^{-1} attributed to C-O-C asymmetric stretch of ether [37, 38]. Fig. 3d

depicts the FTIR spectra of 4-NP after adsorption with JAC. The interaction was clearly noticed due to appearance of a novel peak at 1331 cm^{-1} attributed to N-O stretching. There are also significant shift of peaks from 3399 cm^{-1} to 3424 cm^{-1} corresponding to O-H of phenol, 1038 cm^{-1} to 1036 cm^{-1} and 1111 cm^{-1} to 1107 cm^{-1} due to C-N vibration stretching. All these spectra changes were likely due to adsorption of 4-NP by JAC.

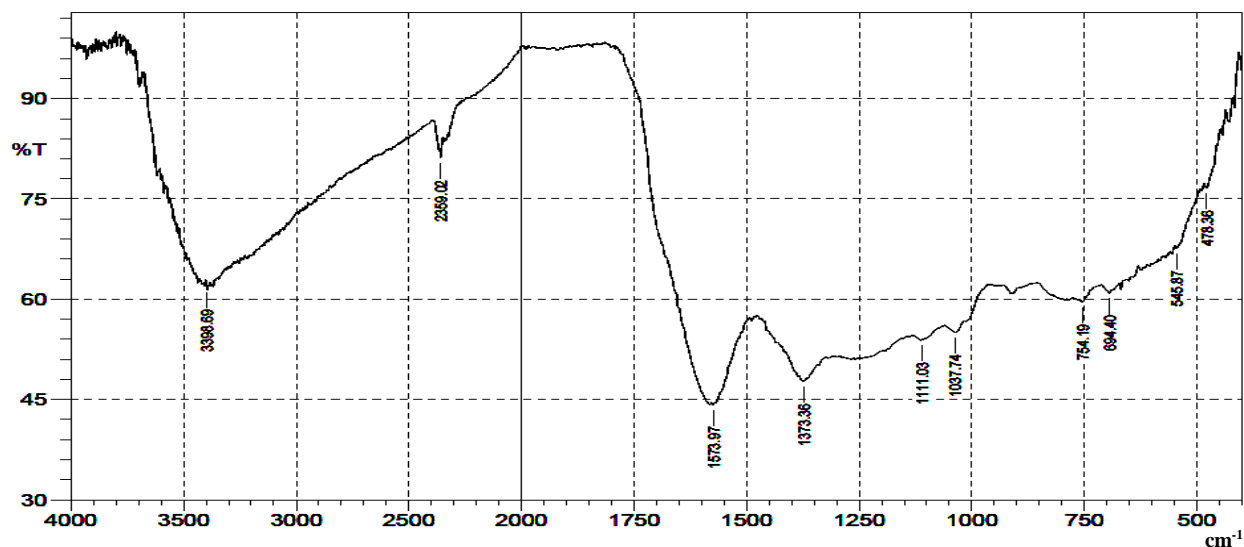


Figure 3c. FTIR spectra of JAC (before adsorption)

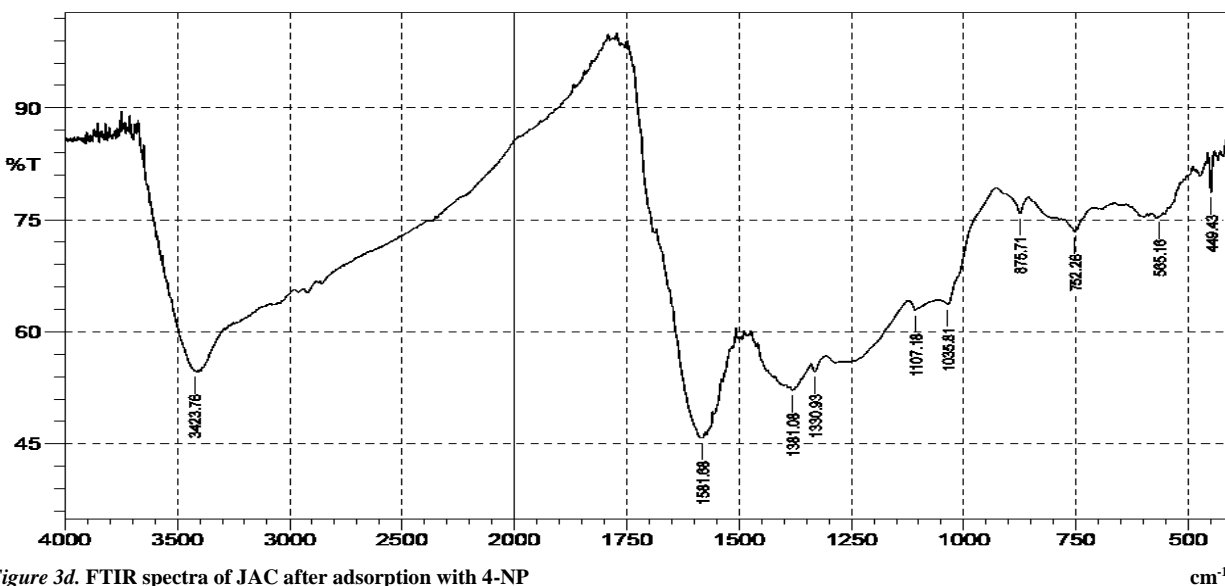


Figure 3d. FTIR spectra of JAC after adsorption with 4-NP

Effect of initial concentration

The percentage removal of 4-NP on both AKC and JAC increases with the concentration as shown in Fig. 4. This shows that the percentage adsorption of 4-NP onto the adsorbents is greatly dependent on initial concentration. The initial 4-NP concentration increased from 10-150 mg/L, the percentage adsorptions at equilibrium were also increased from 68.8 – 74.7% and 67.2 – 81.3% for AKC and JAC respectively. The increase in sorption percentage with increasing 4-NP concentration could be due to higher probability of collision between 4-NP and adsorbents surfaces. Similar observation was earlier reported by Hatem *et al.* [22]. The maximum percentage adsorption onto the adsorbents was found to be 74.7% (3.74 mg/g) and 81% (40.5 mg/g) for AKC and JAC respectively. This shows that JAC is more effective in adsorbing 4-NP than AKC by ten folds [22].

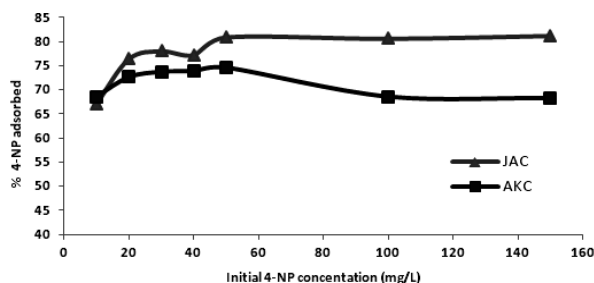


Figure 4. Effect of initial 4-NP concentration uptake onto (a) AKC (w = 0.2 g, pH = 8), (b) JAC (w = 0.02 g, pH = 6), T = 28±2 °C for 2 h at 200 rpm}

Effect of pH

The influence of pH on the removal of 4-NP by AKC and JAC is depicted in Fig. 5. This figure shows that when the pH of the solution was increased from 2 to 5, there was practically no change in the percentage adsorbed for AKC but there was gradual increase for JAC until it reached a plateau at pH of 5. However, when the pH was increased above 5, the removal of 4-NP increased sharply up to 76.42% (3.82 mg/g) at pH 8 for AKC while there was no further increase for JAC after pH of 5. Thus, the adsorption decreases at a very high pH values i.e (pH > 8 for ACK and pH > 6 for JAC). This is because the stability of the neutral molecule of 4-NP is pH dependent. The pKa value of 4-NP is 7.15 being a weak acid [39]. At pH < pKa, the uncharged form of 4-NP is converted into charged species. The graph of pH speciation

diagram for 4-NP actually shows that the conversion of neutral 4-NP into 4-nitrophenolate commences from pH of 5 [40]. The reason could also be due to the electrostatic repulsions between the negatively surface charge of the adsorbents and the 4-nitrophenolate anions in solution. Similar findings were earlier reported by Moreno-Castilla [41]; Atef and Waleed [19].

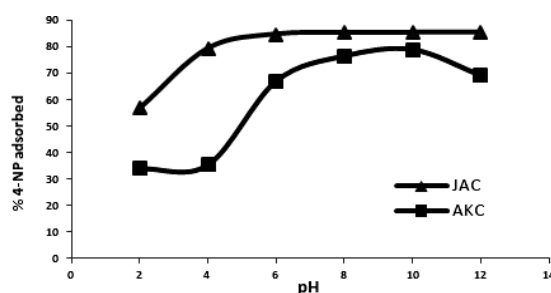


Figure 5. Effect of pH on uptake of 4-NP onto (a) AKC (w = 0.2 g, pH = 8), (b) JAC (w = 0.02 g, pH = 6), Co = 50 mg/L, T = 28±2 °C for 2 h at 200 rpm

Effect of contact time

At the initial stage, the rate of adsorption of 4-NP was very rapid (Fig. 6) as over 70% and 80% of 4-NP were adsorbed in 20 min for AKC and JAC respectively and became slower near the equilibrium time of 120 min. Thereafter, there was no significant change in the quantity and percentage of 4-NP adsorbed. It will also be seen that the amount adsorbed increases with increase in contact time until equilibrium is reached at 120 min for 80.86% (4.05 mg/g)-ACK and 84.66% (42.33mg/g)-JAC. This is similar to the result of Djebbar *et al.* [18]. The saturation curve rises sharply in the initial stages, this is indicative of the fact that there are several available sites to be occupied at the beginning of adsorption process. At plateau region, the adsorbent is saturated at this level [39, 42].

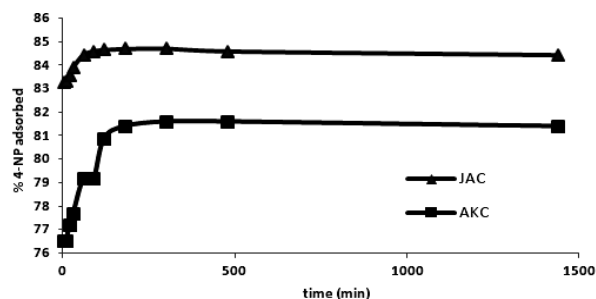


Figure 6. Effect of time on uptake of 4-NP onto (a) AKC (w = 0.2 g, pH = 8), (b) JAC (w = 0.02 g, pH = 6), Co = 50 mg/L T = 28±2 °C for 5 – 1440 min at 200 rpm

Effect of adsorbent dosage

With an increase in the dosage of the AKC (Fig. 7a), only a slight increase in adsorption (35.42–41.64%) was observed while JAC demonstrated a better performance with an increase from 62.26 – 83.56% (Fig. 7b). This could be attributed to increased adsorbent surface area and availability of more sorption sites resulting from the increased adsorbent dosage as observed by Srivastava *et al.* [43].

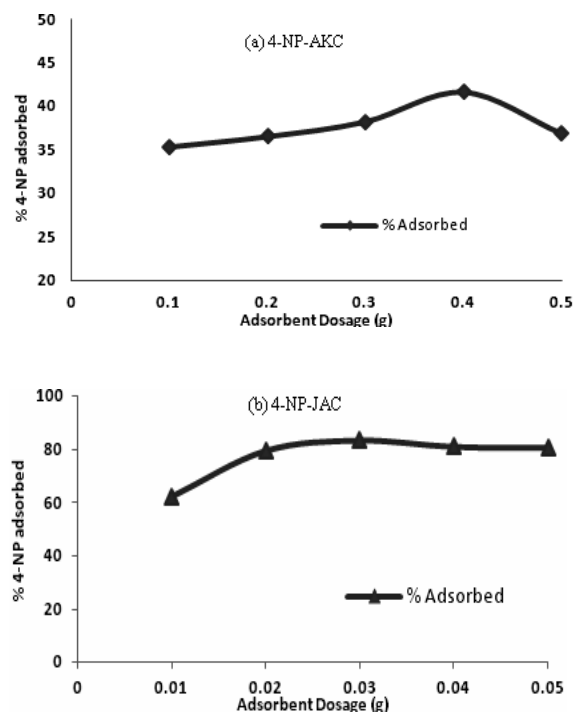


Figure 7. Effect of adsorbent dosage on uptake of 4-NP onto (a) AKC (pH = 8), (b) JAC (pH = 6), $C_o = 50$ mg/L, $T = 28 \pm 2$ °C for 2 h at 200 rpm

Effect of temperature

The adsorption of 4-NP by the adsorbents decrease with increase in temperature (Fig. 8); as the 4-NP removal by AKC and JAC decreased from 44.2–27.6% and 79.64–65.2% respectively. The decrease in percentage adsorbed at higher temperature was due to increase in the solubility of the 4-NP molecules and their diffusion within the pores of the adsorbents as similar observation were earlier reported by Tang *et al.* [39]; Cotoruelo *et al.* [44]; Hatem *et al.* [22]. The decrease in adsorption with increasing temperature signifies an exothermic nature of the entire process.

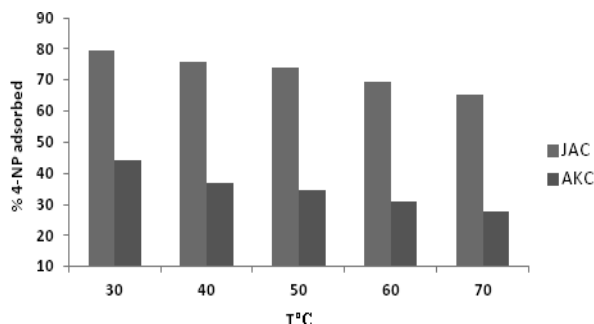


Figure 8. Effect of temperature on uptake of 4-NP onto (a) AKC ($w = 0.2$ g, pH = 8), (b) JAC ($w = 0.02$ g, pH = 6), $C_o = 50$ mg/L, $T = 30 - 70$ °C for 2 h at 200 rpm

Adsorption isotherm

The equilibrium adsorption data of 4-NP on both AKC and JAC were analysed using isotherm models such as Langmuir, Freundlich, Temkin and Dubinin-Radushkevich (D-R). The linear form of the Langmuir equation isotherm can be represented in equation 1 while the heterogeneity of adsorption was deduced from Freundlich equation as presented in Equation 2. Temkin model as represented in equation 3. The linearised equation of Dubinin-Radushkevich (D-R) isotherm is expressed in equation 4 [44].

$$\frac{C_e}{q_e} = \frac{1}{Q_o K_L} + \frac{1}{Q_o} C_e \quad (3)$$

$$\log q_e = \log k_f + \frac{1}{n} \log C_e \quad (4)$$

$$q_e = \frac{RT}{b_T} \ln A_T + \frac{RT}{b_T} \ln C_e \quad (5)$$

$$\ln q_e = \ln q_D - B_D \varepsilon^2 \quad (6)$$

Where C_e is the equilibrium concentration of the adsorbate (mg/L), q_e the amount of adsorbate adsorbed per unit mass of adsorbate (mg/g), Q_o and K_L are Langmuir constants related to adsorption capacity and rate of adsorption, respectively. K_F and n are Freundlich constants, n an indication of how favourable the adsorption process is and K_F is the adsorption capacity of the adsorbent, A_T is Temkin isotherm equilibrium binding constant (L/g), b_T is Temkin isotherm

constant, $B = \frac{RT}{b_T}$ is the constant related to heat of

sorption (J/mol), R is universal gas constant (8.314 J/mol/K), and T is the absolute temperature. q_D is the theoretical isotherm saturation capacity (mg/g), B_D is a constant related to the adsorption energy E (mol²/J²) and ϵ is the Polanyi potential related to the equilibrium concentration as represented by equation 4a and 4b respectively:

$$E = \frac{1}{\sqrt{2B_D}} \quad (6a)$$

$$\epsilon = RT \ln \left[1 + \frac{1}{C_e} \right] \quad (6b)$$

The correlation coefficients of Freundlich isotherms adequately describe the behaviour of 4-NP onto both AKC and JAC as presented in Fig. 9 and in Table 3.

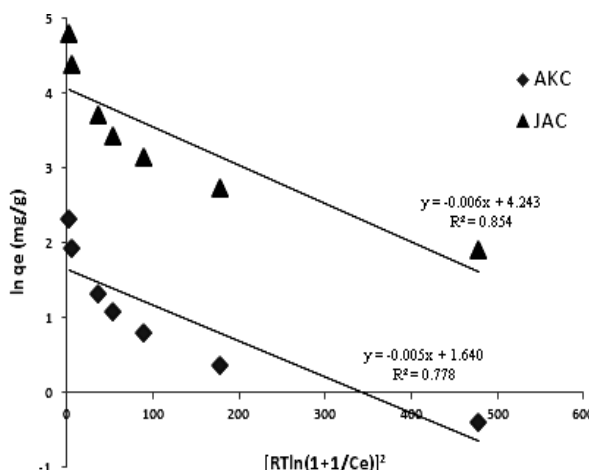
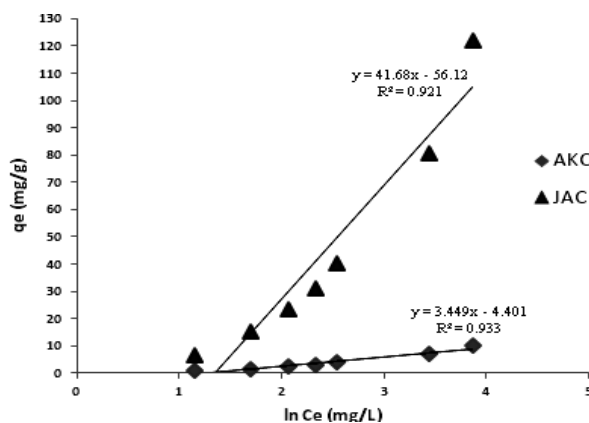
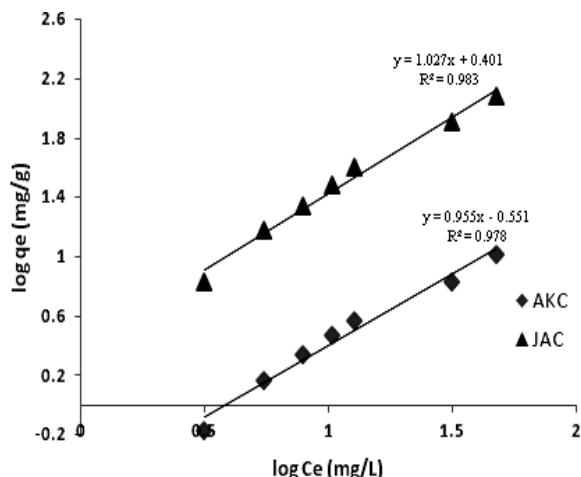
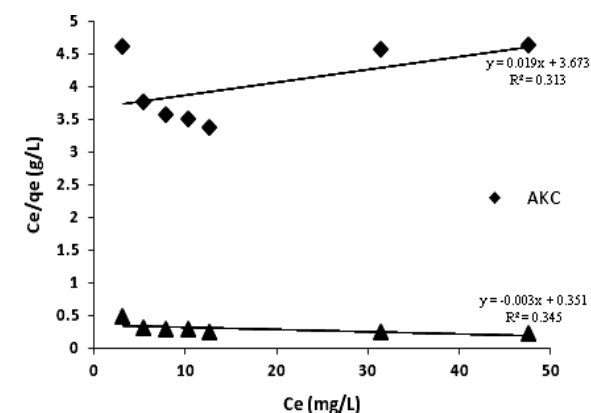


Figure 9. (a) Langmuir; (b) Freundlich; and (c) Temkin; (d) Dubinin-Radushkevich isotherms for the sorption of 4-NP onto AKC and JAC

Table 3. Isotherm parameters for sorption of 4-NP onto AKC and JAC.

Isotherm	Parameters	Values	
		AKC	JAC
Dubinin-Radushkevich	B_D (mol ² /J ²)	5.0×10^{-6}	6.0×10^{-6}
	q_D (mg/g)	5.155	69.616
	E (KJ/mol)	0.316288	0.288675
	R^2	0.778	0.854
Freundlich	K_f (mg/g)	0.281	1.82
	n	1.047	0.775
	R^2	0.978	0.979
Langmuir	R^2	0.313	0.38
Temkin	A (L/g)	0.279	0.266
	B (J/mol)	3.449	52.36
	R^2	0.933	0.917

The values of Freundlich constant n which is 1.047 and 0.775 revealed the favourability of the adsorption process while the constant K_f has a value of 0.281 and 1.82 (mg/g) for both AKC and

JAC respectively, is an indication of a higher adsorption affinity between 4-NP and JAC than AKC. This is due to higher surface area and pore volume of JAC which implies heterogeneity of the adsorption sites. Temkin model with its fairly good correlation coefficients and value of B equals to 3.449 J/mol and 52.36 J/mol for AKC and JAC respectively, revealed that the heat of sorption of 4-NP onto JAC is larger than that of AKC.

Kinetic models

The adsorption kinetics of 4-NP onto AKC and JAC were studied. Four types of kinetic models namely: pseudo-first-order, pseudo-second order, Elovich and Intra-particle diffusion equations were considered to analyse the data of each adsorbents.

The Pseudo-first-order rate expression (Lagergren, 1898) [45] is given as,

$$\ln(q_e - q_t) = \ln q_{e,cal} - \frac{K_1 t}{2.303} \quad (7)$$

The pseudo-second-order kinetic model equation is given as,

$$\frac{t}{q_t} = \frac{1}{K_2 q_{e,cal}^2} + \frac{t}{q_{e,cal}} \quad (8)$$

The Elovich equation is expressed as,

$$q_t = \frac{1}{\alpha} \ln(\alpha\beta) + \frac{1}{\alpha} \ln t \quad (9)$$

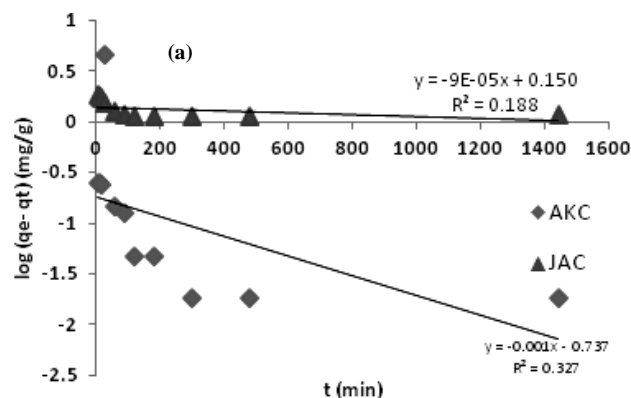
The intra-particle diffusion equation is expressed as:

$$q_t = K_{diff} \sqrt{t} + C \quad (10)$$

Where, q_e (mg/g) and q_t (mg/g) are the amounts of 4-NP adsorbed at equilibrium and at any time t (min), respectively. K_1 (min^{-1}), K_2 ($\text{g}/\text{mg min}$) and K_{diff} ($\text{mg}/\text{g min}^{1/2}$) are the rate constants of the pseudo-first-order, pseudo-second-order and intra-particle diffusion models, respectively. α is the initial adsorption rate ($\text{mg}/\text{g min}$) and β is the

desorption constant (g/mg) during each experiment. C is another constant that gives information about the thickness of the boundary layer [22, 46].

The slope and intercept plot of t/q_t against t (Fig. 10b) were obtained to calculate the second order rate constants K_2 and q_e summarised in Table 4, which shows a good agreement of experimental data with pseudo-second order kinetic model with regression coefficients of 0.999 for both AKC and JAC. It is important to note that the calculated q_e values (4.098 and 43.478 mg/g) for AKC and JAC respectively are in good agreement with their experimental q_e values (4.05 and 40.5 mg/g). This is evident that the pseudo second-order adsorption mechanism was predominant and that the overall rate of the 4-NP adsorption process appeared to be controlled by chemical process. This is similar to observations made by Atef and Waleed [19] and Hatem *et al.* [22]. The intra-particle diffusion constants K_{diff} and C values were evaluated from Figure 10(d-e) and presented in Table 5. The larger intercept values suggest that intra-particle diffusion has a lesser role to play compared with surface diffusion [46]. The figure revealed that two steps occur in the adsorption process. The sharply rising part is the external surface adsorption stage while the second linear part is the gradual adsorption stage where intra-particle or pore diffusion is rate-limiting. The high R^2 values of the sharply rising part suggest that external surface adsorption is the rate-limiting step. The deviation of the lines from the origin and the low R^2 values of the gradual adsorption stage suggest that intra-particle diffusion is not the sole rate limiting step as similar result was earlier reported by Boparai *et al.* [46].



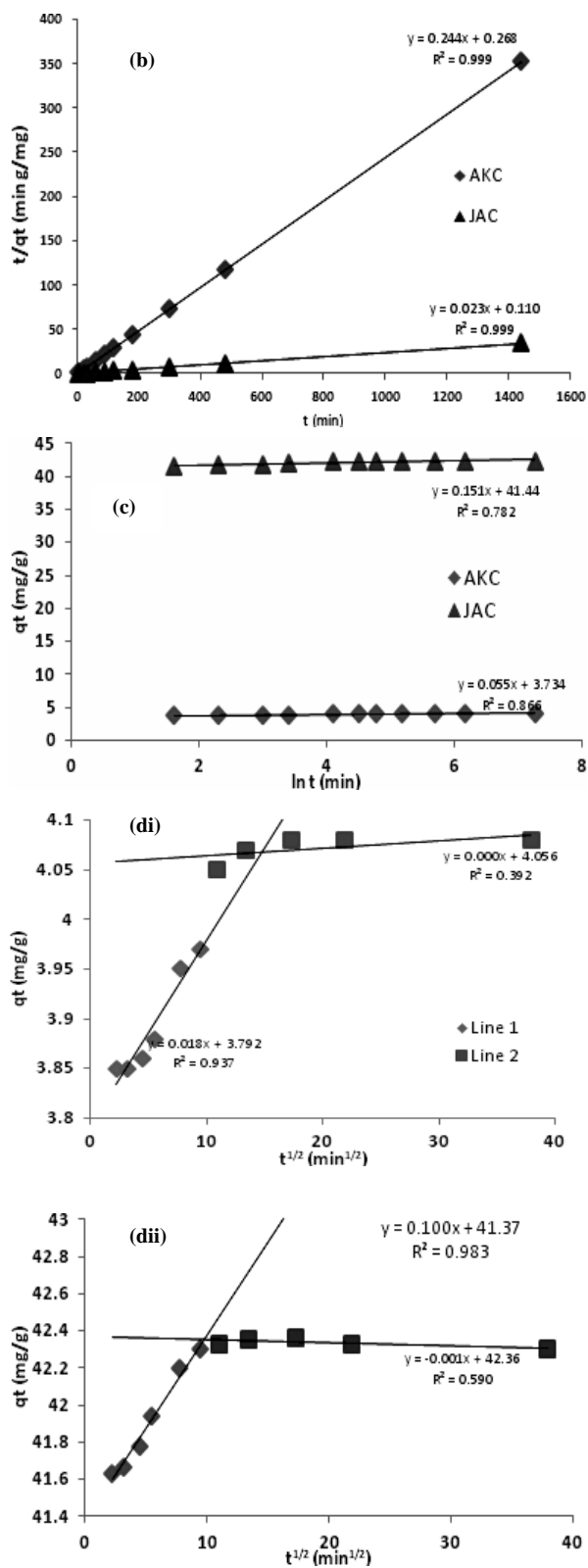


Figure 10. (a) Pseudo-first order; (b) pseudo-second order; and (c) Elovich models for the adsorption of 4-NP onto AKC and JAC. (d) Intra-particle diffusion models for 4-NP onto (i) AKC, (ii) JAC

Table 4. Parameters and correlation coefficients of the kinetic models for 4-NP onto AKC and JAC.

Kinetic Models	Parameters	Values	
		AKC	JAC
Pseudo-first order;	K_1 (min ⁻¹)	2.303×10^{-3}	2.073×10^{-3}
	$Q_{e, cal}$ (mg/g)	0.1833	1.413
	R^2	0.327	0.188
Pseudo-Second order;	K_2 (g/mg/min)	0.222	4.8×10^{-3}
	$Q_{e, cal}$ (mg/g)	4.098	43.478
	$Q_{e, exp}$ (mg/g)	4.05	40.5
	R^2	0.999	0.999
Elovich	α	18.182	6.623
	β	1.681×10^{28}	$e^{-274.457}/6.623$
	R^2	0.866	0.782

Table 5. Parameters and correlation coefficients of the intra-particle diffusion model.

Adsorbents Parameters	AKC		JAC	
	Line 1	Line 2	Line 1	Line 2
K_{diff} (mg/g min ^{1/2})	0.018	0.00	1.085	-0.011
C	3.792	4.056	17.37	29.18
R^2	0.937	0.392	0.967	0.394

Thermodynamic parameters

The thermodynamic parameters such as change in enthalpy (ΔH) and entropy change (ΔS) were estimated from the slopes and intercepts of the linear plots of equation 12, while change in free energy (ΔG) at each temperature were calculated from the obtained values of ΔH and ΔS using Gibb's equation expressed in equation 13 [46].

$$\Delta G = -RT \ln k \quad (11)$$

$$\ln K_c = \frac{\Delta S}{R} - \frac{\Delta H}{RT} \quad (12)$$

$$\Delta G = \Delta H - T\Delta S \quad (13)$$

Where ΔG , ΔH and ΔS are the change in free energy (kJ/mol), enthalpy (kJ/mol), entropy (kJ/mol/ K) respectively. R is the universal gas constant 8.314 (J/mol/K) and T is the adsorption absolute temperature (K). The values of these three parameters (ΔG , ΔH and ΔS) for the sorption of 4-NP onto AKC and JAC are listed in Table 5. As shown in Table 6, the values of the change in enthalpy are negative, signifying that the sorption of 4-NP on both AKC and JAC are exothermic. The adsorption entropy changes

(ΔS) of both adsorbents are negative, which is an indication of the fact that the mobility of adsorbate on the surface of adsorbents is being more restricted in comparison with those in solution. The value of ΔS is lower for AKC ($-0.0687 \text{ kJmol}^{-1}\text{K}^{-1}$) compared to that of JAC ($-0.0376 \text{ kJmol}^{-1}\text{K}^{-1}$). This is due to the fact that the mesopores of JAC are in a more orderly arrangement [47]. The positive values of ΔG for AKC shows that the adsorption process is not feasible and it's not spontaneous, the reaction would have to be induce for it to occur by lowering the temperature of the adsorption process. While that of JAC gives a negative values of ΔG and this confirm the feasibility of the process and the spontaneous nature of the adsorption with a stronger affinity for 4-NP. This is similar to what was earlier reported by Cotoruelo *et al.* [44].

Table 6: Thermodynamic parameters of 4-NP onto AKC and JAC.

	Adsorbents			
	AKC		JAC	
ΔH (kJ/mol)	-14.283		-14.799	
ΔS (kJ/mol/K)	-0.0687		-0.0376	
ΔG (kJ/mol)	T (K)	ΔG	T (K)	ΔG
	303	6.536	303	-3.406
	313	7.22	313	-3.03
	323	7.907	323	-2.654
	333	8.594	333	-2.278
	343	9.281	343	-1.902

Conclusion

For this study, chemical activation method was applied for the preparation of activated Kaolinitic clay and *Jatropha curcas* activated carbon under optimal experimental conditions using HNO_3 and NaOH as the chemical activators respectively. It can be concluded that AKC and JAC are potential and promising adsorbents in the removal of 4-NP from aqueous solution. The results obtained showed that JAC achieved a higher performance compared to AKC for 4-NP removal. The adsorption of 4-NP by AKC and JAC was found to be influenced by the initial concentration of the adsorbates, contact time, solution pH, adsorbent dosage and temperature. Langmuir, Freundlich, Temkin and Dubinin-Radushkevich models were used to examine the adsorption isotherms. Freundlich equation stood out as the best isotherm for describing the

adsorption equilibrium data. The isotherms parameters confirm that the adsorption efficiency of JAC (1.82 mg/g) is higher than that of AKC (0.281 mg/g). Pseudo-second order kinetic model provided the best fit for the experimental data of all the adsorbents. The adsorbed 4-NP decreased with increasing temperature, indicating an exothermic process. The enthalpy changes (ΔH) for the adsorption of 4-NP were all negatives and their absolute values were less than 40 KJ/mol, hence the adsorption is controlled by an exothermic physical process.

References

1. D. N. Jdhav and A. K. Vanjara, *Indian J. Chem. Tech.*, 11 (2004) 35.
2. S. Senel, A. Kara, G. Alsancak and A. Denizli, *J. Hazard. Mater.*, 138 (2006) 317.
3. O. Hamdaoui and E. Naffrechoux, *J. Hazard. Mater.*, 147 (2007) 94.
4. H. G. Franck and J. W. Stadelhofer, *Industrial Aromatic Chemistry*. Springer Verlag, Berlin, (1989) 148.
5. D. C. Greminger, G. P. Burns, S. Lynn, D. N. Hanson and C. J. King, *Ind. Eng. Chem. Process Des.*, 21 (1982) 51.
6. M. Xiao, J. Zhou, Y. Tan, A. Zhang, Y. Xia and L. Ji, *Desalination*, 195 (2006) 281.
7. M. T. A. Reis, O. M. F. De Freitas, M. R. C. Ismael and J. M. R. Carvalho, *J. Membr. Sci.*, 305 (2007) 313.
8. J. Levec and A. Pintar, *A Review. Catal. Today*, 124 (2007) 172.
9. M. Matheswaran, S. Balaji, S. J. Chung and I. S. Moon, *Catal. Commun.*, 8 (2007) 1497.
10. G. Chen, *Sep. Purif. Technol.*, 38 (2004) 11.
11. M. Panizza and G. Cerisola, *Electrochim. Acta*, 51 (2005) 191.
12. M. J. Pacheco, A. Morao, A. Lopes, L. Ciriaco and I. Goncalves, *Electrochim. Acta*, 53 (2007) 629.
13. D. Rajkumar and K. Palanivelu, *J. Hazard. Mater.*, B113 (2004) 123.
14. P. Saravanan, K. Pakshirajan and P. Saha, *Bioresour. Technol.*, 99 (2008) 205.
15. K. Nazari, N. Esmaeili, A. Mahmoudi, H. Rahimi and A. A. Moosavi-Movahedi, *Enzyme Microb. Technol.*, 41 (2007) 226.
16. Y. Ku and K. C. Lee, *J. Hazard. Mater.*, B80 (2000) 59.

17. O. S. Fatoki, O. S. Ayanda, F. A. Adekola and B. J. Ximba, *Clean Soil Air Water*, 42 (2013) 472.
18. M. Djebbar, F. Djafri, M. Bouchekara and Djafri, *Afr. J. Pure Applied Chem.*, 6 (2012) 15.
19. S. A. Atef and M. Waleed, *Int'l. J. Phys.*, 4 (2009) 172.
20. S. Preeti and B. K. Singh, *Indian J. Chem.*, 46A (2007) 620.
21. H. I. Adegoke and F. A. Adekola, *Adv. Natural and Appl. Sci.*, 4 (2010) 293. ISSN 1995-0748.
22. A. A. Hatem, M. J. Maah, R. Yahyar and M. Radzi bin abas, *Asian J. Chem.*, 25 (2013) 9575.
23. W. A. Deer, R. A. Howie and J. Zussman, *An introduction to the rock forming minerals*. Second edition Harlow: Longman, ISBN 0-582-30094-0 (1992).
24. W. L. Pohl, *Economic geology, principles and practice; metals, mineral, coal and hydrocarbons- Introduction to formation and sustainable exploitation of mineral deposits* Wiley Blackwell, 331, ISBN 978-1-4443-3662-7 (2011).
25. H. M. Hadyn, "Industrial application of kaolin" Georgia Kaolin Company, Elizabeth, New Jersey. Tenth National Conference on Clays and Clay Minerals (1955).
26. J. Janick, and E. P. Robert, *The Encyclopaedia of Fruit & Nuts*. CABI. 371–372. ISBN 978-0-85199-638-7 (2008).
27. W. M. J. Achten, E. Mathijs, L. Verchot, V.P. Singh, R. Aerts and B. Muys B., *Jatropha biodiesel fuelling sustainability Biofuels, Bioproducts and Biorefining*. 1 (2007) 283.
28. K. Nahar and M. Ozores-Hampton, *Jatropha an Alternative Substitute to Fossil Fuel* (IFAS Publication Number HS1193). Gainesville: University of Florida, Institute of Food and Agricultural Sciences (2011).
29. A. Qadeer and A. Rehan, *Turk J. Chem.*, 26 (2002) 357.
30. O. A. Ekpete, A. I. Spiff, M. Horsfall Jr. and P. Adowei, *Innov. Sci. Eng.*, 2 (2012) 7.
31. T. A. Adebayo and O. Ajayi, *Asian Transactions on Eng.*, 1 (2011) 2221.
32. O. S. Olokode and P. O. Aiyedun, *Pacific J. of Sci. and Technol.*, 12 (2011) 558.
33. S. Tangjuank, N. Insuk, J. Tontrakoon and V. Udeye, *World Acad. Sci., Eng. Technol.*, 52 (2009) 110.
34. S. Karthikeyan, K. Sakthivel and C. Kannan, *Rasayan J. Chem.*, 4 (2011) 519.
35. A. Gadsden, *Infrared Spectra of Minerals and Related Inorganic Compounds*. The Butterworth group, UK, (1975).
36. J. Madejova, *Vibrational Spectroscopy*, (2003) 311.
37. M. S. Islam, M. A. Rouf, S. Fujimoto and T. Minowa, *Bangladesh J. Sci. Ind. Res.*, 47 (2012) 257..
38. W. Tongpoothor, M. Sriuttha, P. Homchan, S. Chanthai and C. Ruangviriyachai, *Chem. Eng. Res.Des.*, 89 (2011) 335.
39. D. Tang, Z. Zheng, K. Lin, J. Luan and J. Zhang, *J. Hazard. Mater.*, 143 (2007) 49.
40. I. Diaconu, R. Girdea, C. Camelia, N. Gheorghe, R. Elena and E. E. Totu, *Romanian Biotechnol. Letters*, 15 (2010) 5702.
41. C. Moreno-Castilla, *Carbon*, 42 (2004) 83.
42. M. Uddin, M. Islam and M. Abedin, *ARPN J. Eng. Appl. Sci.*, 2 (2007) 11.
43. V. C. Srivastava, M. M. Swammy, I. D. Mall, B. Prasad and I. M. Mishra, *Colloids Surf. A Physicochem Eng. Aspects*, 272 (2006) 89.
44. L. M. Cotoruelo, M. D. Marques, F. J. Diaz, J. Rodriguez-Mirasol, J.J. Rodriguez and T. Cordero, *Chem. Eng. J.*, 184 (2012) 176.
45. Lagergren S., *Handlingar*, 24 (1898) 1.
46. K. H. Boparai, J. Meera and M. O. Denis, *J. Hazard Mater.*, 186 (2011) 458.
47. L. Ai-min, W. Hai-suo, Z. Quan-xing, Z. Gen-cheng, L. Chao, F. Zheng-hao, L. Fu-qiang and C. Jin-long, *Chinese J. Polymer Sci.*, 22 (2004) 259.